Angiotensin-II and MARCKS

*A HYDROGEN PEROXIDE- AND RAC1-DEPENDENT SIGNALING PATHWAY IN VASCULAR ENDOTHELIUM**

Hermann Kalwa[1], **Juliano L. Sartoretto**, **Simone M. Sartoretto**, and **Thomas Michel**[2]

From the Cardiovascular Division, Department of Medicine, Brigham and Women's Hospital, Harvard Medical School, Boston, Massachusetts 02115

Background: The role of the actin-binding protein MARCKS in angiotensin-II signaling is unknown.

Results: Biochemical and cell imaging approaches establish that angiotensin-II promotes Rac1- and H_2O_2-dependent MARCKS phosphorylation and cytoskeleton rearrangement.

Conclusion: MARCKS plays a critical role in angiotensin-II signaling.

Significance: Angiotensin-II is implicated in vascular physiology and pathophysiology; these studies identify MARCKS as a key determinant of angiotensin-II-modulated responses in the vascular endothelium.

MARCKS is an actin-binding protein that modulates vascular endothelial cell migration and cytoskeleton signaling (Kalwa, H., and Michel, T. (2011) *J. Biol. Chem.* 286, 2320–2330). Angiotensin-II is a vasoactive peptide implicated in vascular physiology as well as pathophysiology; the pathways connecting angiotensin-II and cytoskeletal remodeling are incompletely understood. Here we show that MARCKS is expressed in intact arterial preparations, with prominent staining of the endothelium. In endothelial cells, angiotensin-II-promoted MARCKS phosphorylation is abrogated by PEG-catalase, implicating endogenous H_2O_2 in the angiotensin-II response. Studies using the H_2O_2 biosensor HyPer2 reveal that angiotensin-II promotes increases in intracellular H_2O_2. We used a Rac1 FRET biosensor to show that angiotensin-II promotes Rac1 activation that is attenuated by PEG-catalase. siRNA-mediated Rac1 knockdown blocks angiotensin-II-stimulated MARCKS phosphorylation. Cell imaging studies using a phosphoinositide 4,5-bisphosphate (PIP_2) biosensor revealed that angiotensin-II PIP_2 regulation depends on MARCKS and H_2O_2. siRNA-mediated knockdown of MARCKS or Rac1 attenuates receptor-mediated activation of the tyrosine kinase c-Abl and disrupts actin fiber formation. These studies establish a critical role for H_2O_2 in angiotensin-II signaling to the endothelial cytoskeleton in a novel pathway that is critically dependent on MARCKS, Rac1, and c-Abl.

The MARCKS[3] (myristoylated alanine-rich C kinase substrate) protein was first described more than 20 years ago as a

neuronal phosphoprotein that binds calmodulin (1). The expression of MARCKS has since been documented in many different mammalian cells and tissues (1–6). A general understanding of MARCKS phosphorylation has emerged over the years through analyses of the purified MARCKS protein (1, 3, 8) and studies of MARCKS dynamics in cultured cells (4–7, 9–14). In resting cells, MARCKS associates with the plasma membrane and plasmalemmal caveolae via the protein polybasic domains and by its specific interactions with the signaling phospholipid phosphatidylinositol-(4,5)-diphosphate (PIP_2, Refs. 3, 8, 10). Phosphorylation of MARCKS takes place on serine and threonine residues in the protein polybasic domain. Phosphorylated MARCKS undergoes translocation to intracellular sites, where the protein interacts with actin. Phosphorylation of MARCKS also inhibits its binding to calmodulin. The robust and dynamic interactions between MARCKS and these key signaling/structural molecules help to form the basis for the protein broad effects on cellular function. Indeed, the phosphorylation of MARCKS has been implicated in neuronal development (5, 9) and in the migration of vascular endothelial cells (7, 12) and neurons (14). The MARCKS[null] knock-out mouse is embryonic lethal (9, 11, 13), and no tissue-specific mouse knock-out models have been described. Much about the receptor-dependent modulation of MARCKS phosphorylation and its implications for vascular cell function remains incompletely understood.

The vasoactive peptide angiotensin-II (Ang-II) has critical roles both in normal vascular physiology as well as in vascular disease states (see reviews in Refs. 15–18). Ang-II has been most extensively characterized in vascular smooth muscle cells, where its effects on vascular tone and oxidative stress are primarily modulated by G protein-coupled AT1 receptors. Less completely characterized are the effects of Ang-II on vascular endothelial cells, where the hormone appears to have both short- and long-term effects on endothelial function. Ang-II appears to modulate endothelial cell motility and to increase

---

[3] The abbreviations used are: MARCKS, the myristoylated alanine-rich C kinase substrate protein; H_2O_2, hydrogen peroxide; ROS, reactive oxygen species; PI3K, phosphatidylinositol 3-kinase; Ang-II, angiotensin-II; PKC, protein kinase C; PIP_3, phosphatidylinositol 3,4,5-trisphosphate; PIP_2, phosphatidylinositol 4,5-bisphosphate; vWF, von Willebrand factor; siRNA,

small interfering RNA; FRET, fluorescence resonance energy transfer; BAEC, bovine aortic endothelial cell.
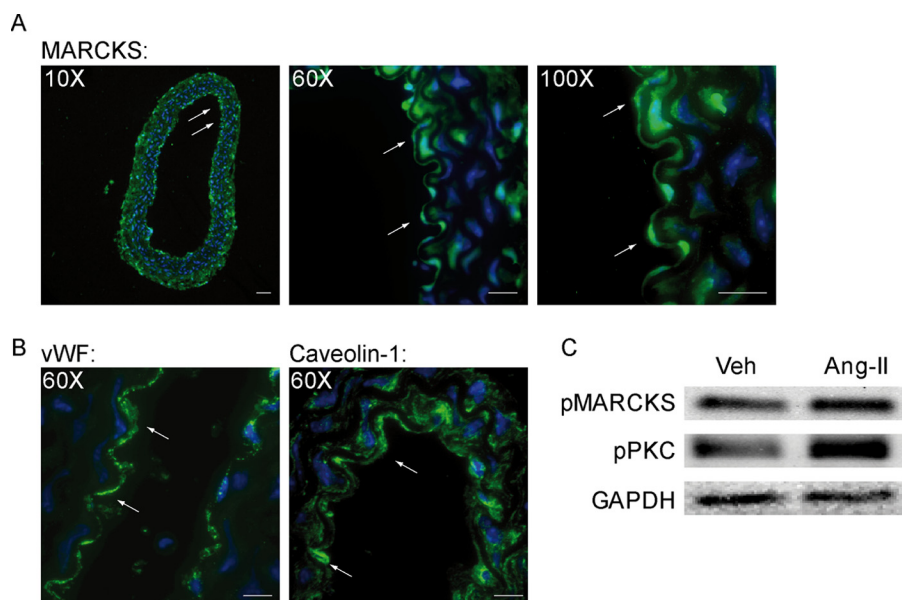
FIGURE 1. **MARCKS expression and phosphorylation in arterial preparations.** *Panels A* and *B* show representative photomicrographs of murine carotid artery preparations that were fixed, paraffin-embedded, and stained with antibodies against MARCKS, vWF and Caveolin-1 respectively, followed by staining with a secondary antibody conjugated to Alexa Fluor 488. Nuclei were stained with 4,6-diamidino-2-phenylindole (*DAPI*). Intrinsic fluorescence was diminished by preincubation with Pontamine sky blue as described (48). Images were obtained by white light confocal imaging (magnification ×10 - 100). *Panel C* shows an immunoblot of freshly-isolated murine aortic preparations that were incubated for 15 min with Ang-II (500 nM) and then probed with phosphospecific antibodies directed against MARCKS and PKC; GAPDH serves as a loading control. These results are representative of three similar experiments that yielded similar findings.

the intracellular generation of reactive oxygen species (17, 19). A recent study has implicated the endothelial cell AT1 receptor for Ang-II in the development of aortic aneurysms (20), yet much remains to be learned about the signaling pathways involved in endothelial Ang-II signaling and pathological responses in endothelial cells.

The present studies continue our ongoing exploration of the role of MARCKS in endothelial cell biology. We have previously shown that siRNA-mediated MARCKS knockdown in cultured endothelial cells effectively abrogates directed cell migration and leads to marked changes in the endothelial cytoskeleton (12). These observations have lead to our current studies on the role and regulation of MARCKS in signaling pathways initiated by Ang-II. Activation by Ang-II of the AT1 receptor leads to the stimulation of protein kinase C, one of the key protein kinases that phosphorylates MARCKS (2). Activation of the AT1 receptor also leads to marked changes in cytoskeletal structure and to increases in the intracellular levels of reactive oxygen species (ROS) such as hydrogen peroxide (H_2O_2, reviewed in Refs. 15–18). ROS have long been characterized as deleterious compounds that are implicated in inflammation, neurodegeneration, and aging (21, 22). It is now clear that the stable ROS H_2O_2 also plays a central role in physiological signaling pathways in a variety of cells and tissues. The present studies provide evidence for a pathway linking Ang-II-dependent H_2O_2 generation to MARCKS phosphorylation via a signaling pathway that involves the key cytoskeleton-associated proteins Rac1 and c-Abl. These observations establish new connections between signaling pathways that previously were largely studied in isolation, and provide new insights into the roles of the enigmatic MARCKS protein in the vascular endothelium. These findings may have implications for our understanding of the physiological and pathological responses to Ang-II.

EXPERIMENTAL PROCEDURES

Reagents—FBS was purchased from HyClone Laboratories. All other cell culture reagents, media, and Lipofectamine 2000 were from Invitrogen. FuGENE 6 transfection reagent was from Roche Applied Science. phorbol 12-myristate 13-acetate was from Calbiochem. Antibodies directed against MARCKS, Phospho MARCKS, phospho c-Abl, Rac1, and vinculin were from cell signaling. Alexa Fluor 488- and Alexa Fluor 568-coupled secondary antibodies and phalloidin/Alexa Fluor 568 were from Invitrogen. SuperSignal chemiluminescence detection reagents and secondary antibodies conjugated with HRP were from Pierce. The FRET biosensor plasmids were the kind gift of Professor Matsuda, University of Kyoto (33). All other reagents were from Sigma.

siRNA Design—On the basis of established characteristics of siRNA-targeting constructs, we designed a c-Abl duplex siRNA with the sequence 5′-CAG ACG AAG UGG AAA AGG AdTdT-3′. We used previously characterized and validated duplex siRNA targeting constructs for MARCKS (12) and Rac1 (32). The RNA sequence used as a negative control in siRNA transfections was 5′-GCG CGC UUU GUA GGA UUC G-dTdT-3′. All duplex siRNA-targeting constructs were purchased from Ambion.

Cell Culture and Transfection—Bovine aortic endothelial cells (BAEC) were obtained from Genlantis (San Diego, CA) and maintained in culture in Dulbecco's modified Eagle's medium supplemented with fetal bovine serum (10%, v/v) as described previously. Cells were plated onto gelatin-coated culture dishes and studied prior to cell confluence between passages 6 and 8. siRNA transfections were performed as described previously. Briefly, 24 h after cells were split at a 1:8 ratio, and duplex siRNA constructs (final concentration 30 nM) were
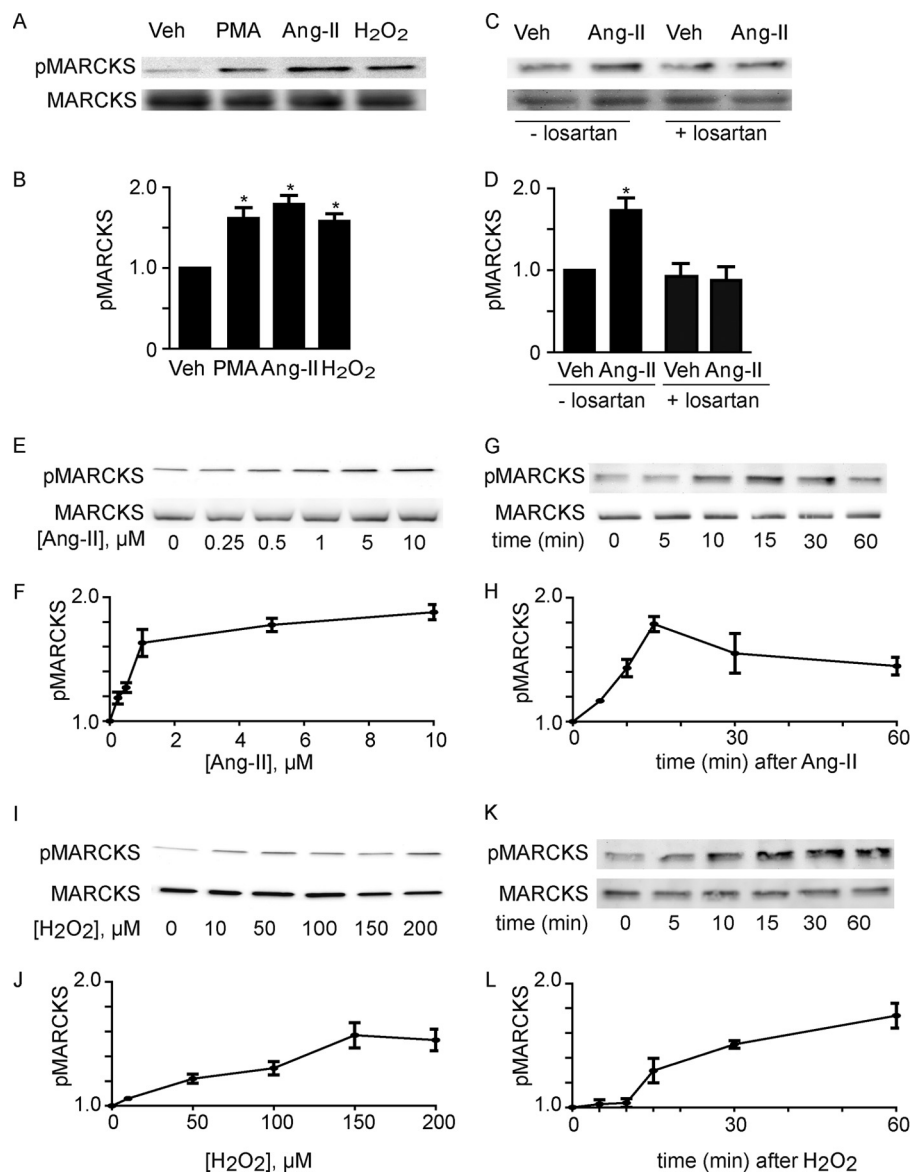
FIGURE 2. **Angiotensin-stimulated MARCKS phosphorylation in endothelial cells.** *Panel A* shows a representative immunoblot of endothelial cells that were incubated for 15 min with phorbol ester PMA (10 nM), Ang-II (500 nM), or H_2O_2 (100 μM), and probed with phospho-MARCKS (pMARCKS) or total MARCKS antibodies. Quantitative analyses of pooled data from four similar experiments are shown below in *panel B*; the * indicates $p < 0.05$ by ANOVA. *Panel C* shows representative immunoblots analyzed in endothelial cells that were pre-incubated with the AT1 receptor antagonist losartan (or vehicle) and then exposed to Ang-II (500 nM, 15 min) or vehicle (*veh*), and probed with antibodies as shown; quantitative analyses of pooled data from 4 similar experiments are shown below in *panel D. Panels E–L* present the results of dose response and time course experiments exploring Ang-II or H_2O_2-mediated MARCKS phosphorylation responses in endothelial cells. Lysates prepared from treated endothelial cells were resolved by SDS-PAGE and analyzed in immunoblots probed with antibodies as shown. In the time course experiments, cells were treated with either 100 μM hydrogen peroxide or 500 nM angiotensin-II; in the dose response experiments, cells were analyzed 15 min after addition of agonists. Representative immunoblots are shown as well as quantitative analyses derived from pooled data; each point in the graphs represents the mean $\pm$ S.E. of three independent experiments. The *asterisk* * indicates $p < 0.05$ analyzed by ANOVA.

transfected using Lipofectamine 2000 (0.15%, v/v), following the protocol provided by the manufacturer. Lipofectamine 2000 was then removed by changing into fresh medium containing 10% FBS 5 h after transfection. Plasmid transfection was carried out with Lipofectamine at a ratio of 1:3 (w/v) according to the manufacturer's protocol. For combined transfections of siRNA-targeting constructs plus plasmid cDNA, the siRNA was transfected first as described above. 5 h after siRNA transfection, the medium was replaced, and the DNA mixture was added and incubated with the cells overnight, at which point the medium was replaced again. Cells were analyzed for a total of 48 h following siRNA transfections.

Cell Treatments and Immunoblot Analyses—Angiotensin II was dissolved in H_2O and stored at -20 °C. PMA was dissolved in dimethyl sulfoxide and stored at -20 °C. After drug treatments, lysates from BAEC were prepared using a cell lysis buffer (50 mM Tris-HCl, pH 7.4, 150 mM NaCl, 1% Nonidet P-40, 0.025% sodium deoxycholate, 1 mM EDTA, 2 mM Na_3VO_4, 1 mM NaF, 2 μg/ml leupeptin, 2 μg/ml antipain, 2 μg/ml soybean trypsin inhibitor, and 2 μg/ml lima trypsin inhibitor). Immunoblot analyses of protein expression and phosphorylation were performed as described previously. Detection and quantitation of immunoblots were performed using a ChemiImager HD4000 (AlphaInnotech, San Leandro, CA).
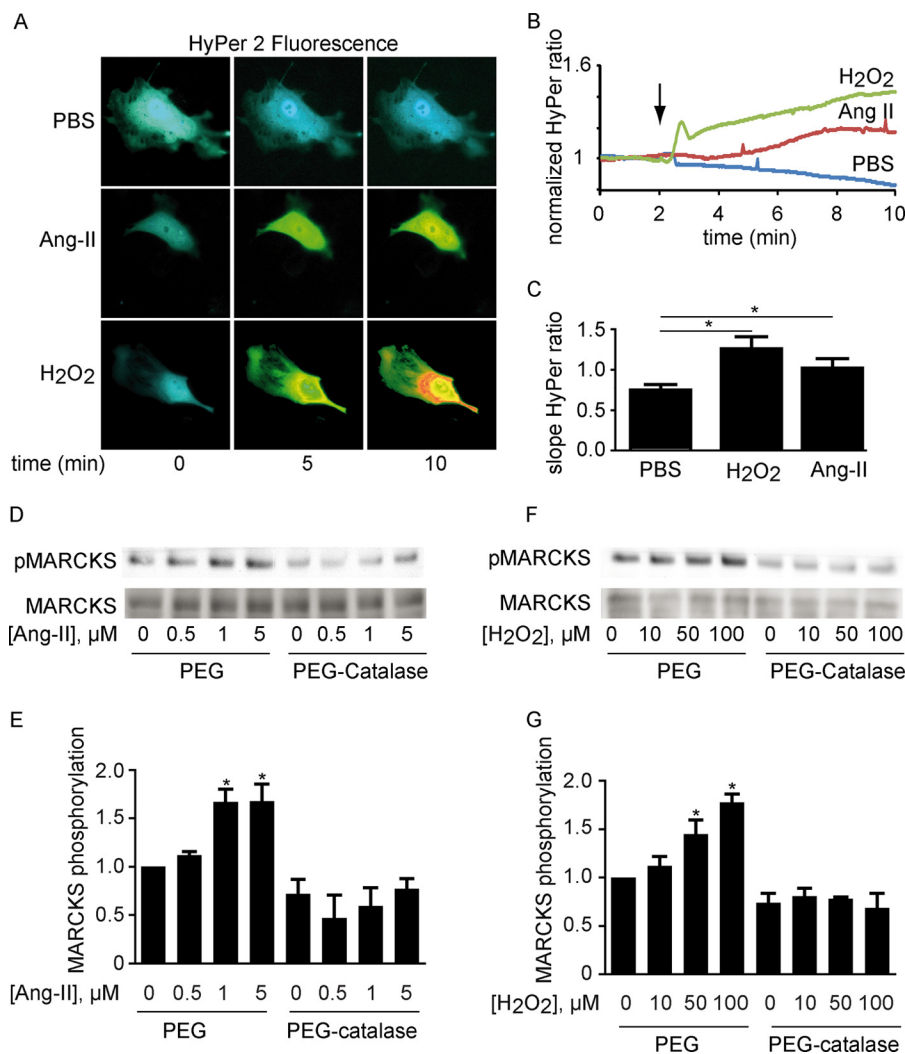
FIGURE 3. **Role of H$_2$O$_2$ in Ang-II-promoted MARCKS phosphorylation.** Endothelial cells were infected with a lentivirus expressing the HyPer2 biosensor for H$_2$O$_2$; shown are representative images (*panel A*) as well as fluorescence tracings (*panel B*) following cell treatments with PBS, Ang-II (500 nM), or H$_2$O$_2$ (100 μM). The HyPer2 signal was entirely blocked by pre-treatment with PEG-catalase (not shown), as we have previously reported (49). *Panel C* shows the quantitative analyses of data pooled from 4 similar experiments, measuring the HyPer2 fluorescence ratio determined 8 min after agonist addition; the asterisk * indicates $p < 0.05$ by ANOVA. As we previously In *panels D* and *E*, endothelial cells were pre-incubated with either PEG or PEG-catalase, and then treated with either Ang-II (500 nM), H$_2$O$_2$ (100 μM) or vehicle; immunoblots were then probed with antisera specific for phosphorylated or total MARCKS. Shown above are representative immunoblots; the graphs below present the quantification of pooled data from 4 similar experiments. The *asterisk* * indicates results significant at $p < 0.05$ compared with $t = 0$, analyzed by ANOVA.

HyPer2 Lentivirus Cloning and Analysis—The coding sequence of HyPer2 was cloned into the pWPXL lentiviral expression plasmid downstream of the EF1-α promoter. Recombinant vesicular stomatitis virus-glycoprotein pseudotyped lentivirus particles were generated in HEK293T cells by transfection of the envelope:packaging:transgene plasmids at a 1:1:1.5 ratio with Fugene6 (Roche) according to the manufacturer's protocol. The viral titer was determined with Lenti-X GoStix (Clontech), and virus particles were concentrated by polyethylene glycol precipitation with PEG-it solution (SBI Bioscience), according to the manufacturer's protocol. The virus pellet was resuspended in PBS and stored at −80 °C. Final titer was determined by serial dilution and fluorescence microscopy.

Fluorescence Microscopy—HyPer2 fluorescence was excited with 420/40 and with 500/16 band-pass excitation filters; corresponding YFP. Emission was acquired every 5 s for 15 min using a 535/30 band-pass emission filter. For calculating HyPer

ratio images were acquired; after background subtraction, the HyPer2 signal was quantitated as we and others have previous reported (45). For analyses of fixed cells, BAEC grown on glass-bottomed dishes (Mattek, Boston, MA) or on glass coverslips were treated as indicated, fixed with 4% paraformaldehyde in PBS for 10 min, rinsed with PBS, permeabilized in 0.1% Triton X-100 in PBS for 5 min, and blocked with 10% goat serum in PBS for 1 h. Incubations with primary antibodies were performed in blocking solution for 1 h at room temperature or in the cold room overnight. After washing with PBS, cells were incubated with appropriate secondary antibodies conjugated to immunofluorescent dyes (Alexa Fluor 488 anti-mouse IgG or Alexa Fluor 568 anti-rabbit IgG) in blocking solution for 1 h at room temperature. After washing three times with PBS, cover slips were mounted on slides using medium containing 4′,6-diamidino-2-phenylindole as nuclear counter stain. Microscopic analysis of samples was performed using an Olympus

IX81 inverted microscope in conjunction with a DSU spinning disk confocal system equipped with a Hamamatsu Orca ER cooled-CCD camera. Images were acquired using a $100\times/1.4$ differential interference contrast oil immersion objective lens and analyzed using MetaMorph software (Universal Imaging, Downingtown, PA).

F-Actin Visualization—F-Actin was stained with phalloidin/ AlexaFluor-568 (InVitrogen, San Diego, CA). Cells were fixed and permeabilized as described above, and then incubated with phalloidin/AlexaFluor-568 (100 nM) for 30 min. Microscopic analysis of samples was performed using an Olympus DSU spinning disk confocal system. Images were acquired using a $60\times$ or $100\times$ differential interference contrast oil immersion objective lens and analyzed using MetaMorph.

Determination of Fluorescence Resonance Energy Transfer (FRET)—All live cell FRET imaging experiments were carried out in HEPES-buffered saline (HBSS, containing 140 mM NaCl, 6 mM KCl, 1.25 mM $MgCl_2$, 2 mM $CaCl_2$, 10 mM HEPES, and 5 mM glucose, pH 7.4. Monitoring of FRET was performed using methods described in detail previously (12, 30, 31, 33, 34, 46, 47). In brief, BAEC were transiently transfected with a plasmid encoding the FRET biosensors. Upon activation, this molecular construct undergoes a structural change that leads to an increase in FRET ratio. Excitation of CFP-PH was at 425 ± 10 nm, and emission was collected at 475 ± 10 (CFP) and 540 ± 10 nm (YFP) using the Semrock FRET-CFP/YFP-B 4-filter single-band set. A series of fluorescence images were taken at 60 s time intervals; visualization and analysis was performed using the MetaMorph FRET module. All FRET construct were kind gifts of Professor Michiyuki Matsuda, Department of Tumor Virology, Research Institute for Microbial Diseases, Kyoto University, Japan.

Other Methods—All experiments were performed at least three times. Mean values for experiments were expressed as mean $\pm$ S.E. Statistical differences were assessed by analysis of variance. A p value less than 0.05 was considered statistically significant.

RESULTS

To document the expression of MARCKS in the vascular wall, paraffin sections of murine carotid arteries were stained with a MARCKS-specific antibody and analyzed by fluorescence microscopy (Fig. 1*A*). The endothelial cell layer was identified by immunostaining with antibodies directed against von Willebrand factor (vWF) and caveolin-1 (Fig. 1*B*). Robust MARCKS protein staining is seen in the endothelial cell layer, as well as some MARCKS staining in the underlying smooth muscle cells. We next analyzed immunoblots of murine aortic preparations treated *ex vivo* with Ang-II, and found that Ang-II enhances MARCKS phosphorylation concomitant with an increase in protein kinase C phosphorylation. To further delineate the signaling pathways connecting Ang-II and MARCKS, we pursued studies in cultured endothelial cells using the well-characterized bovine aortic endothelial cells (BAEC) model system. As shown in Fig. 2, *A* and *B*, incubation of BAEC with the PKC activator phorbol 12-myristate 13-acetate (PMA) leads to marked increases in MARCKS phosphorylation. Treatment of BAEC with either Ang-II or H_2O_2 also promotes a striking
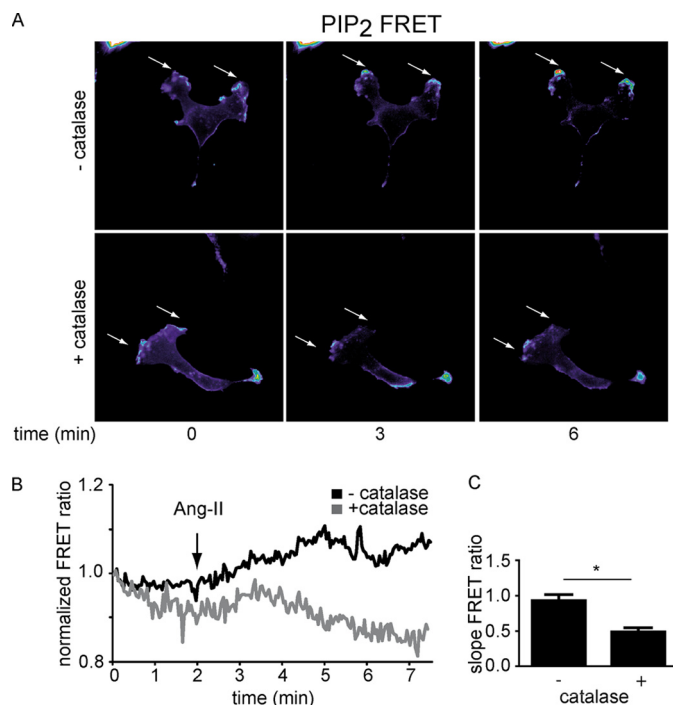

FIGURE 4. **Angiotensin-II-stimulated localized increases in PIP$_2$ are blocked by PEG-catalase.** *Panel A* shows representative images of endothelial cells that had been transfected with the PIP$_2$ biosensor PiPi and then incubated with either PEG or PEG-catalase, followed by treatment with Ang-II (500 nM) for the indicated times. The individual panels show representative time lapse photomicrographs of cells analyzed for FRET; real-time quantitation of the FRET ratio for these images is shown in *panel B*. *Panel C* shows pooled quantitative data from six independent experiments. The data are expressed as change of FRET ratio determined 8 min after addition of Ang-II; the *asterisk* * indicates $p < 0.05$ by t test.

increase in MARCKS phosphorylation. We next performed dose-response and time course experiments for MARCKS phosphorylation stimulated by H_2O_2 or Ang-II, and analyzed immunoblots probed with phosphospecific antibodies. These experiments, shown in Fig. 2, document the dose- and time-dependent phosphorylation of MARCKS in response to Ang-II (Fig. 2, *E–H*) or H_2O_2 (Fig. 2, *I–L*). Importantly, the AT1 receptor antagonist losartan blocks Ang-II-induced phosphorylation of MARCKS (Fig. 2, *C* and *D*).

These observations help to establish that Ang-II and H_2O_2 elicit similar effects on MARCKS phosphorylation in endothelial cells. Since Ang-II has been implicated in ROS synthesis in many cell types, we next sought to explore the effects of Ang-II on intracellular H_2O_2 levels in endothelial cells (17, 23, 24). We used the well-characterized H_2O_2 biosensor HyPer2 (25–27), which we have previously generated as a recombinant lentiviral construct and used to monitor cellular H_2O_2 levels (28). We infected BAEC with the HyPer2 lentivirus, and then treated the cells with Ang-II and analyzed the H_2O_2 response in real time by ratiometric live cell imaging. As shown in Fig. 3, *A–C*, Ang-II treatment promotes a significant increase in the HyPer2 signal; H_2O_2 treatment serves as a positive control. These observations provide strong evidence for an Ang-II-promoted increase in endogenous levels of H_2O_2 in these cells. Further evidence for a central role for endogenous H_2O_2 in Ang-II-dependent signal transduction comes from experiments using the membrane-permeable H_2O_2– degrading enzyme PEG-catalase. As shown
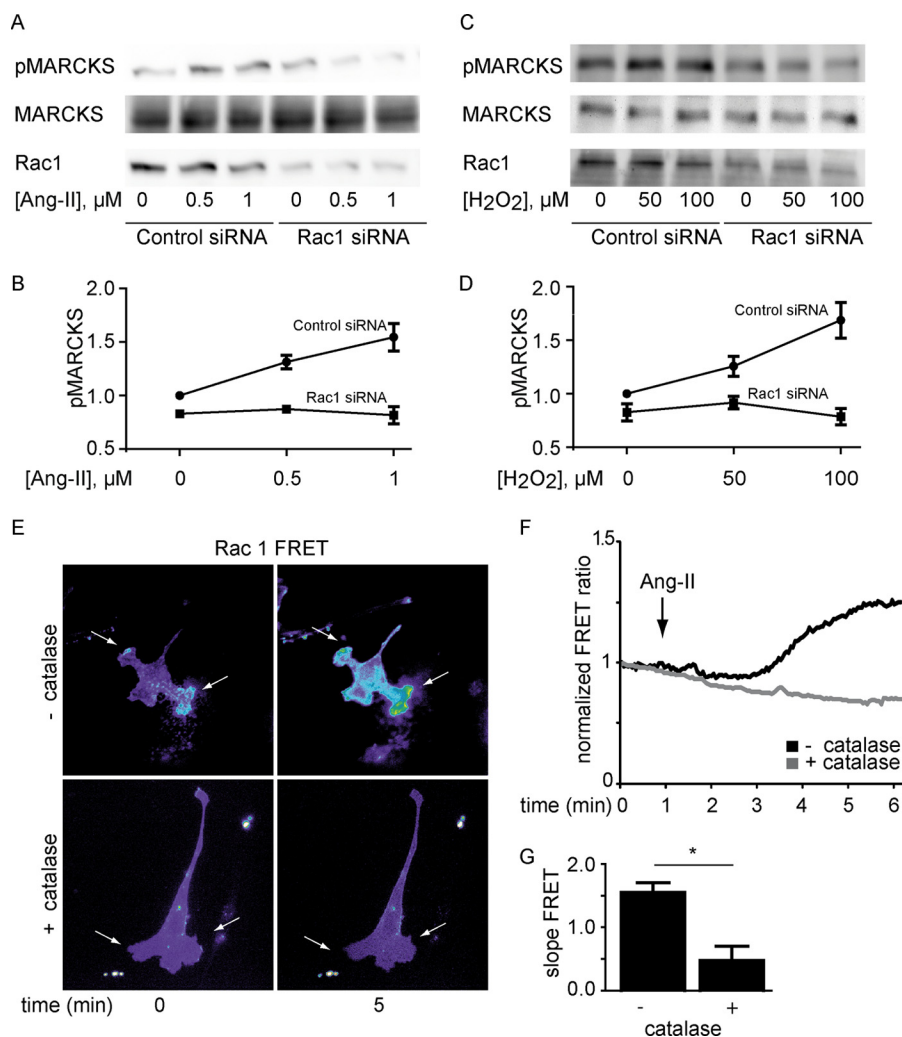
FIGURE 5. **Ang-II-modulated Rac1 activation and the role of H_2O_2.** In *panels A–D*, endothelial cells were transfected with control or Rac1 siRNA, treated for 15 min with the indicated concentrations of Ang-II or H_2O_2, and analyzed in immunoblots probed with antibodies against phospho-MARCKS (pMARCKS), total MARCKS, or Rac1, as indicated. Representative immunoblots are shown in *panels A* and *C*, and the corresponding quantitative analyses of data pooled from 4 independent experiments are shown in *panels B* and *D*; the *asterisk* indicates $p < 0.05$ by ANOVA. In *panels E–G*, endothelial cells were transfected with the Rac1 biosensor plasmid Raichu-Rac1 and then treated with either PEG or PEG-catalase and analyzed by FRET live cell imaging following addition of Ang-II (500 nM). *Panel E* shows time lapse photomicrographs from a representative experiment. *Panels F* and *G* present pooled quantitative data from five independent experiments. In *panel F*, the data are expressed as change of normalized FRET ratio over time, reflecting the activation of Rac1 at the plasma membrane. *Panel G* shows the slope of the FRET ratio determined 6 min after addition of Ang-II as analyzed in five independent experiments (13 cells total); the *asterisk* * signifies $p < 0.05$.

in Fig. 3, *D* and *E* and *F* and *G*, after incubating BAEC with PEG-catalase, Ang-II treatment no longer stimulates any increase in MARCKS phosphorylation; again, H_2O_2 serves as a positive control. In some experiments, PEG-catalase led to a small decrease in basal MARCKS phosphorylation, but this effect was not statistically significant, perhaps reflecting variability in the levels of basal MARCKS phosphorylation in these cells. Taken together, these observations suggest that Ang-II-stimulated H_2O_2 serves as a key intracellular mediator linking AT1 receptor activation to MARCKS phosphorylation in endothelial cells.

The signaling phospholipid PIP_2 is another critical MARCKS binding partner (2, 6, 8, 12, 29). MARCKS phosphorylation leads to the dissociation of MARCKS and PIP_2 at the cell membrane (2). We exploited the highly specific PIP_2 FRET biosensor PiPi (30, 31) to explore the role of H_2O_2 in Ang-II-stimulated PIP_2 metabolism. The PiPi biosensor changes its fluorescence characteristics in response to alterations in local phospholipid composition. BAEC were transfected with cDNA encoding the PiPi biosensor and the cells were then analyzed by live cell imaging after stimulation with Ang-II. As shown in Fig. 4, Ang-II treatment leads to localized increases in PIP_2 at cellular protrusion zones. The Ang-II-promoted increase in localized PIP_2 abundance is completely abolished by preincubation of the cells with PEG-catalase (Fig. 4), again implicating H_2O_2 as a critical determinant of the cellular response to Ang-II.

Alterations in cellular protrusion zones often accompany changes in the activity of cytoskeleton-associated Rho GTPases, particularly Rac1 (31). Moreover, it is well established that Rac1 activity can be enhanced by activation of AT1 receptors (24). To test the involvement of Rac1 in MARCKS signaling in endothelial cells, we "knocked down" Rac1 using a highly specific siRNA targeting construct that we have extensively
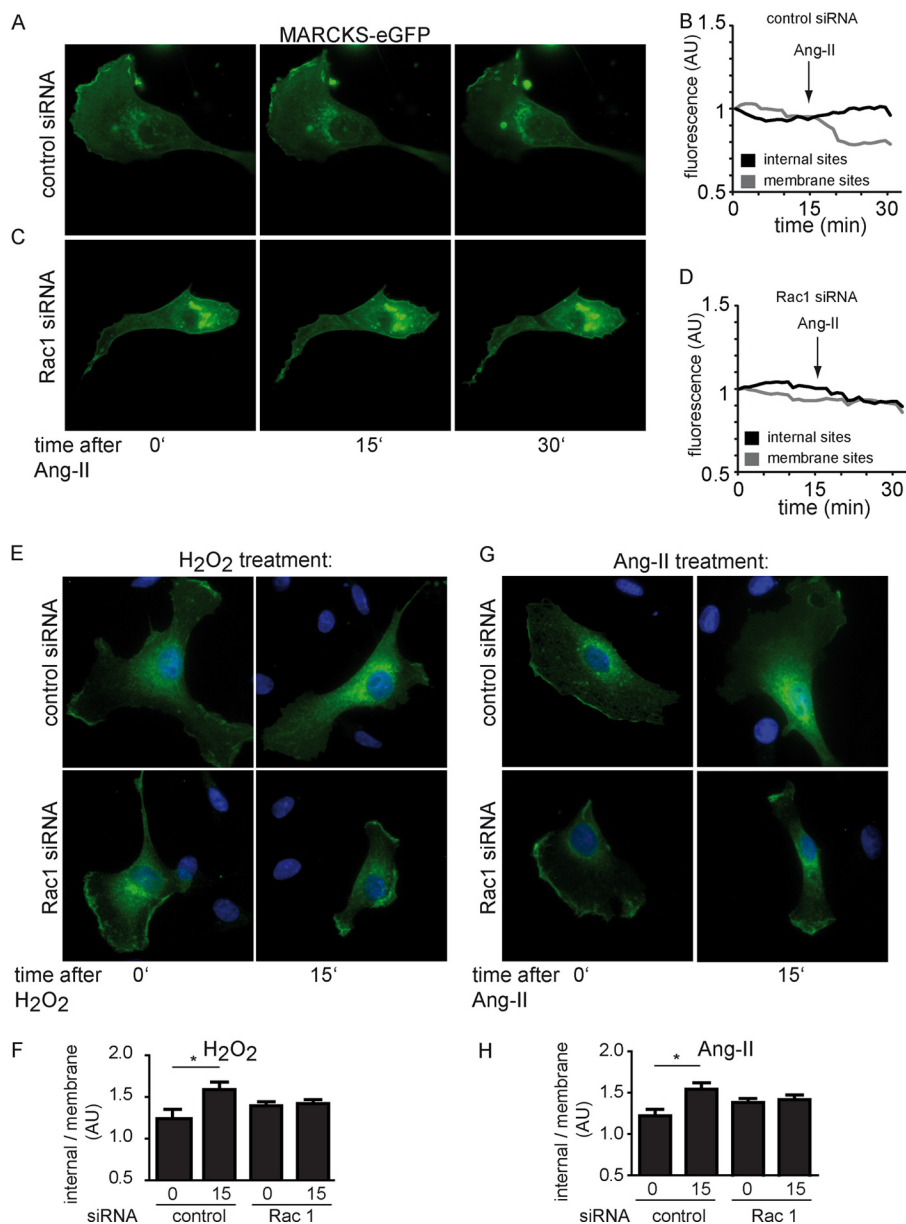
FIGURE 6. **Effects of siRNA-mediated Rac1 knockdown on MARCKS translocation.** Endothelial cells were co-transfected with a cDNA construct encoding a MARCKS-eGFP fusion protein along with either control or Rac1 siRNA. Transfected cells were analyzed by live cell imaging following the addition of Ang-II (500 nM), H_2O_2 (100 μM), or vehicle, as indicated. Fluorescence at peripheral and internal sides was monitored and displayed as the change in normalized fluorescence over time. *Panels A–D* show a time course of representative live cell images, and *panels E* and *G* show still images from fixed cells that were acquired after 15 min of incubation with Ang-II (500 nM), H_2O_2 (100 μM), or vehicle. Quantitative plots of fluorescence at peripheral and internal sides was analyzed from the pooled data (*panels F* and *H*). Each value represents the mean ± S.E. from three independent experiments that yielded similar results. *, $p = 0.05$.

characterized in BAEC in previous studies (32). siRNA-mediated Rac1 knockdown completely abrogates the MARCKS phosphorylation response seen after angiotensin II or H_2O_2 stimulation (Fig. 5, *A–D*). We next explored whether endogenous H_2O_2 is required for Rac1 activation in experiments using a Rac1 FRET biosensor called Raichu-Rac1 (33–35). We transfected BAEC with Raichu-Rac1 cDNA and then treated these cells with Ang-II; live cell imaging showed that Ang-II promotes a robust increase of the Raichu-Rac1 FRET ratio (Fig. 5, *E–G*). This Ang-II-promoted increase in Raichu-Rac1 FRET ratio is blocked by PEG-catalase, again indicating a central role for H_2O_2 in Ang-II-dependent Rac1 activation. Because Rac1 activation can promote marked changes in cytoskeletal struc-

ture, we explored the effects of siRNA-mediated Rac1 knockdown on the subcellular localization of MARCKS. MARCKS localization was analyzed in BAEC transfected with a cDNA encoding eGFP-tagged MARCKS. As shown in Fig. 6, MARCKS in resting cells is visualized both in peripheral and internal membranes. Treatment with Ang-II leads to the translocation of MARCKS away from peripheral membranes to intracellular locations, as seen in time lapse images and quantified by monitoring changes in relative fluorescence at the membrane and internal sites (Fig. 6). Live cell imaging of MARCKS localization (Figs. 6, *A–D*) used wide-field microscopy, whereas confocal imaging approaches were used in the studies of fixed cells (Fig. 6, *E–H*). After siRNA-mediated Rac1
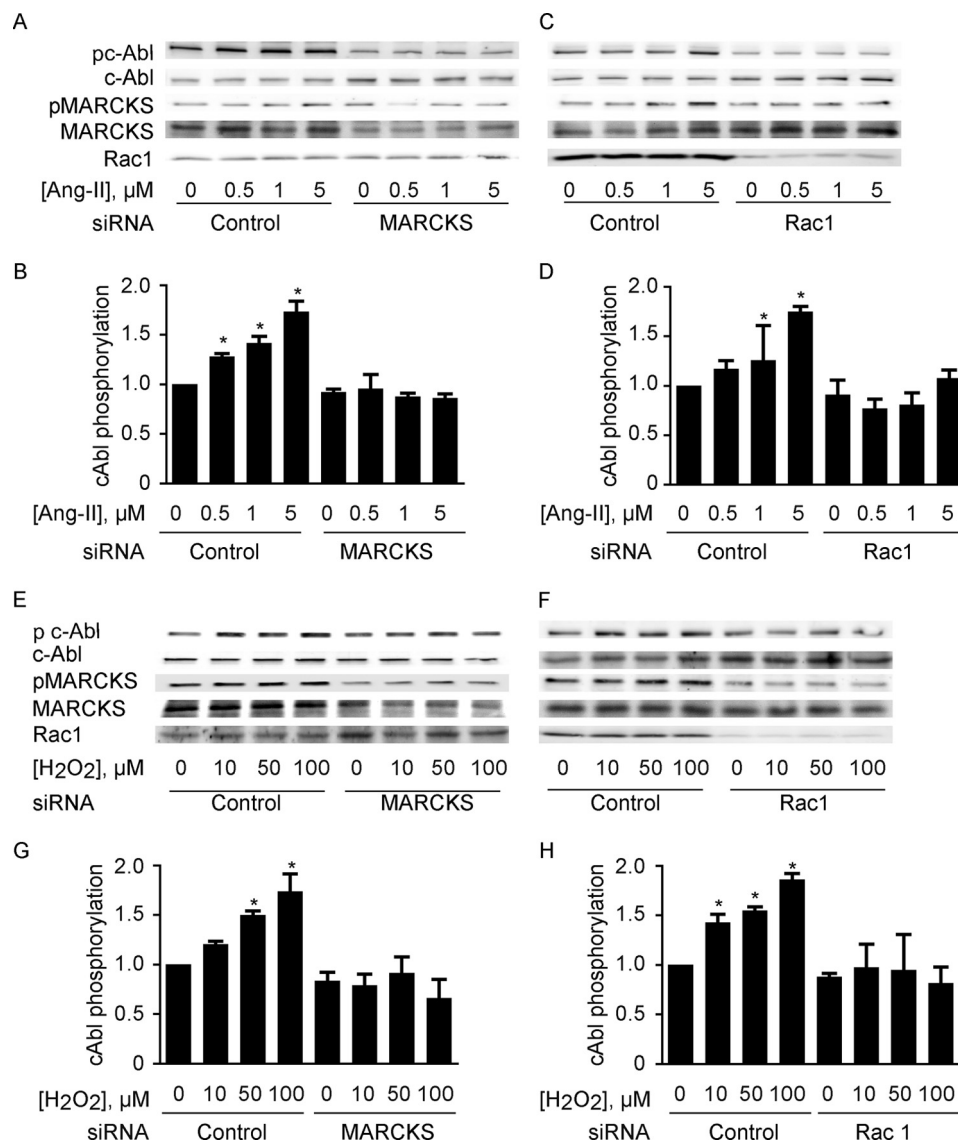
FIGURE 7. **Ang-II-promoted phosphorylation pathways are modulated by Rac1 and MARCKS.** Shown are immunoblots from dose-response experiments in endothelial cells were transfected either with control siRNA or with siRNA targeting constructs for MARCKS and Rac1 then treated for 15 min with Ang-II (500 nM, *panels A–D*) or H_2O_2 (100 μM, *panels E–H*) and probed with antibodies directed against phosphorylated or total c-Abl, phosphorylated or total MARCKS, or Rac1, as indicated. Representative immunoblots are shown in *panels A, C, E,* and *F*; quantitative analyses of pooled data are shown in *panels B, D, G,* and *H*. Each bar in the graphs represents the mean ± S.E. of four independent experiments that yielded similar results. * indicates $p < 0.05$.

knockdown, there is an increase in the relative abundance of cytosolic MARCKS, and Ang-II elicits no further change in MARCKS localization. The effects of siRNA-mediated Rac1 knockdown on MARCKS localization were also analyzed using confocal imaging in fixed cells to improve spatial resolution and permit more rigorous quantitation (Fig. 6, *E–H*); these studies verified the results of live cell imaging.

These findings of Ang-II-modulated regional PIP_2 dynamics, Rac1 activation, and MARCKS translocation together strongly implicate cytoskeletal rearrangements as a key component of the Ang-II response. One of the most important steps of cytoskeletal rearrangement is activation of the tyrosine kinase c-Abl (36–39). As shown in Fig. 7, incubation of BAEC with either H_2O_2 or Ang-II leads to an increase in c-Abl phosphorylation at Tyr-245, a site that has been associated with c-Abl activation (40). The Ang-II- or H_2O_2-promoted increase in c-Abl phosphorylation is blocked by siRNA-mediated knockdown of

either MARCKS or Rac1 (Fig. 7). In contrast, siRNA-mediated knockdown of c-Abl effectively abrogated Ang-II- or H_2O_2-promoted MARCKS phosphorylation (Fig. 8). Finally, we investigated the role of the cytoskeletal protein vinculin in this pathway. Vinculin directly interacts with PIP_2, and vinculin immunostaining serves as a robust marker for the formation of focal adhesion complexes (41). Fig. 9 shows analyses of focal adhesion complex formation in BAEC using confocal imaging to detect vinculin immunofluorescence in combination with phalloidin staining for filamentous actin. Both Ang-II and H_2O_2 promote a significant increase in focal adhesion sites as well as an increase in cytoskeletal stress fibers. As shown in Fig. 9, after siRNA-mediated knockdown of either Rac1, MARCKS, or cAbl, vinculin staining reveals a disordered pattern of focal adhesion sites, and neither Ang-II nor H_2O_2 promote a substantive response, in marked contrast to control siRNA-treated cells.
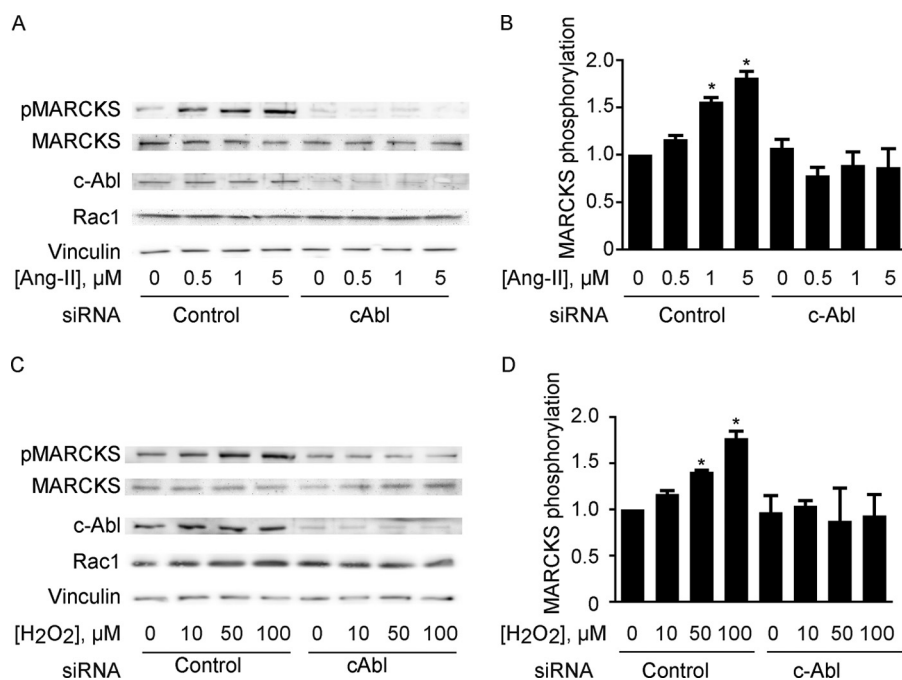
FIGURE 8. **siRNA-mediated knockdown of c-Abl attenuates Ang-II mediated MARCKS phosphorylation.** Shown are immunoblots from dose-response experiments in endothelial cells were transfected either with control siRNA or with a siRNA targeting constructs specific for c-Abl then treated for 15 min with Ang-II (500 nM, *panels A-B*) or H_2O_2 (100 μM, *panels C-D*) and then probed with antibodies directed against total c-Abl, phosphorylated or total MARCKS, Rac1, or vinculin as indicated. Representative immunoblots are shown in *panels A* and *C*; quantitative analyses of pooled data are shown in *panels B* and *D*. Each bar in the graphs represents the mean ± S.E. of four independent experiments that yielded similar results. * indicates $p < 0.05$.

DISCUSSION

The principal finding of these studies is that Ang-II promotes the H_2O_2- and Rac1-dependent phosphorylation and translocation of the actin-binding protein MARCKS in vascular endothelial cells, leading to phosphorylation of the c-Abl tyrosine kinase and to cytoskeleton rearrangement (see the model in Fig. 10). We found that MARCKS is expressed and dynamically phosphorylated in the arterial wall, with particularly robust MARCKS expression in the vascular endothelium (Fig. 1). We discovered that MARCKS phosphorylation in cultured vascular endothelial cells is stimulated by Ang-II via the AT1 receptor, as shown by the abrogation of the Ang-II response by the AT1 receptor antagonist losartan (Fig. 2). Our studies have used live cell imaging with highly sensitive and specific biosensors to document the effects of Ang-II on the intracellular accumulation of H_2O_2 (Fig. 3) and of PIP_2 (Fig. 4), and also to establish the Ang-II-dependent activation of the key signaling proteins Rac1 (Figs. 5 and 6) and c-Abl (Fig. 7). The intimate connections between these signaling pathways were revealed by studies using well-characterized siRNA targeting constructs to "knock down" Rac1, MARCKS, and c-Abl. These studies revealed that siRNA-mediated Rac1 knockdown effectively abrogated Ang-II signaling to MARCKS (Fig. 5) or c-Abl (Fig. 7). Clearly, there is a dynamic reciprocal relationship between c-Abl and MARCKS, in that siRNA-mediated knockdown of MARCKS attenuates c-Abl phosphorylation, and conversely siRNA-mediated knockdown of c-Abl blocks MARCKS phosphorylation. This interaction between MARCKS and c-Abl may facilitate the coordination of discrete receptor-dependent phosphorylation pathways that modulate key cytoskeleton responses.

These studies have also presented several lines of evidence implicating endogenous H_2O_2 as the critical determinant of Ang-II-stimulated signaling responses in endothelial cells. Studies using the H_2O_2 biosensor HyPer2 provide direct evidence that Ang-II leads to an increase in intracellular H_2O_2 levels (Fig. 3). Experiments exploiting the cell-permeable reagent PEG-modified catalase to degrade intracellular H_2O_2 showed that PEG-catalase completely abrogates Ang-II-stimulated MARCKS phosphorylation (Fig. 3) as well as the Ang-II-dependent increase in localized PIP2 accumulation (Fig. 4). Activation of the AT1 receptor can lead to localized increases in ROS (17, 24); in turn, ROS have been implicated in rearrangement of the actin cytoskeleton (15, 22). The specific molecular target(s) that modulate the effects of H_2O_2 on MARCKS-regulated cellular responses have not been identified in these studies. Indeed, there are many H_2O_2–modulated pathways that could be involved in the altered MARCKS-dependent responses that we have observed following H_2O_2 treatment. For example, there are many protein kinases and phosphoprotein phosphatases that are regulated by H_2O_2 (16, 21–23), or the H_2O_2-dependent oxidation of the MARCKS protein itself might lead to changes in its phosphorylation state and alter signaling to the endothelial cytoskeleton.

The involvement of H_2O_2 in dynamic actin reorganization and adhesion led us to test the potential role of vinculin in these cells. Vinculin is a highly conserved and abundant protein involved in linking the actin cytoskeleton to the cell membrane at sites of cellular adhesion. At sites of cell adhesion, vinculin plays a role in physiological processes such as cell motility, migration, development, and wound healing (42). Loss of normal vinculin function has been associated with invasive cancer
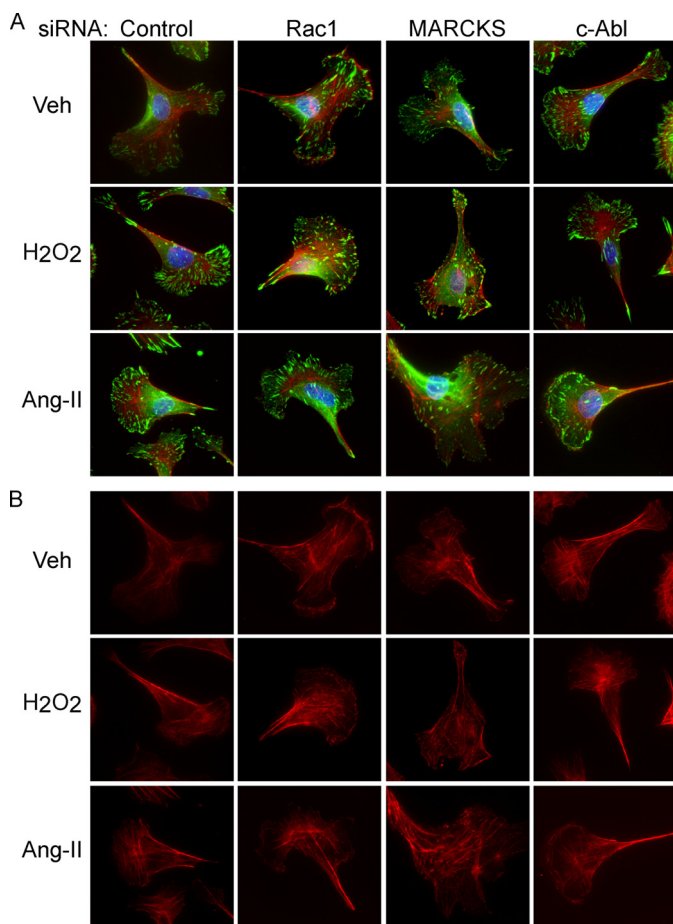
FIGURE 9. **siRNA-mediated knockdown of Rac1, MARCKS or c-Abl leads to disruption of focal adhesion sites in endothelial cells.** Endothelial cells were transfected with control siRNA or with siRNA constructs targeting Rac1, MARCKS, or c-Abl, as shown. Cells with treated with vehicle (control), Ang-II (500 nM), or H_2O_2 (100 μM)) for 15 min, and then fixed and stained. Filamentous actin (F-Actin) was labeled with Alexa 568 phalloidin (*red*), and vinculin was stained using with a vinculin antibody following a secondary antibody coupled to Alexa 488 (*green*).

FIGURE 10. **Model of Ang-II signaling to the endothelial cytoskeleton via MARCKS and H_2O_2.** This scheme shows that the Ang-II-dependent activation of the AT1R receptor in vascular endothelila cells leads to Rac1 activation and to increased levels of H_2O_2, both of which are required for MARCKS phosphorylation and cytoskeleton responses. The AT1R blocker losartan blocks downstream Ang-II-stimulated signaling responses. siRNA-mediated knockdown of Rac1 attenuates Ang-II-stimulated MARCKS phosphorylation and translocation, as does the enzymatic degradation of H_2O_2 after PEG-catalase treatment. MARCKS phosphorylation leads to increased levels of free PIP_2 and to the translocation of phospho-MARCKS from the membrane to internal sites, where phosphorylated MARCKS binds actin and promotes formation of adhesion complexes containing vinculin. siRNA-mediated knockdown of cAbl attenuates MARCKS phosphorylation, implicating this protein kinase in the pathway modulating MARCKS phosphorylation. Conversely, siRNA-mediated knockdown of MARCKS leads to an attenuation of c-Abl phosphorylation, suggesting reciprocal regulatory interactions between these two signaling proteins. Taken together, these observations help to establish a central role for MARCKS in Ang-II signaling in the vascular endothelium.

phenotypes, cardiovascular disease states, and derangements in embryogenesis that are also present in the embryonic lethal MARCKS knock-out mouse (9, 11, 42, 43). Importantly, the tail domain of vinculin binds to acidic phospholipids, predominantly PIP_2. It has been proposed that PIP_2 plays a role in vinculin activation and focal adhesion turnover (44). In control cells stained for vinculin and F-actin, stimulation with Ang-II or H_2O_2 leads to an increase in focal adhesion complexes and organized fiber formation. The loss of MARCKS, Rac1, or c-Abl, respectively drives the cytoskeleton into a hyperactivated, dysregulated state comparable to agonist stimulation, which then appears to be unresponsive to further increase. This fits nicely into the previous findings, that cells lacking MARCKS having difficulties establishing and stabilizing directed movement (12).

Studies in vascular smooth muscle cells have concluded that the increases in intracellular ROS levels elicited by Ang-II involve the AT1 receptor-dependent activation of NADPH oxidase isoforms involving Rac1 (17, 23). However, the signaling pathways connecting AT1 receptor activation and ROS accumulation in endothelial cells are less well understood. Indeed,
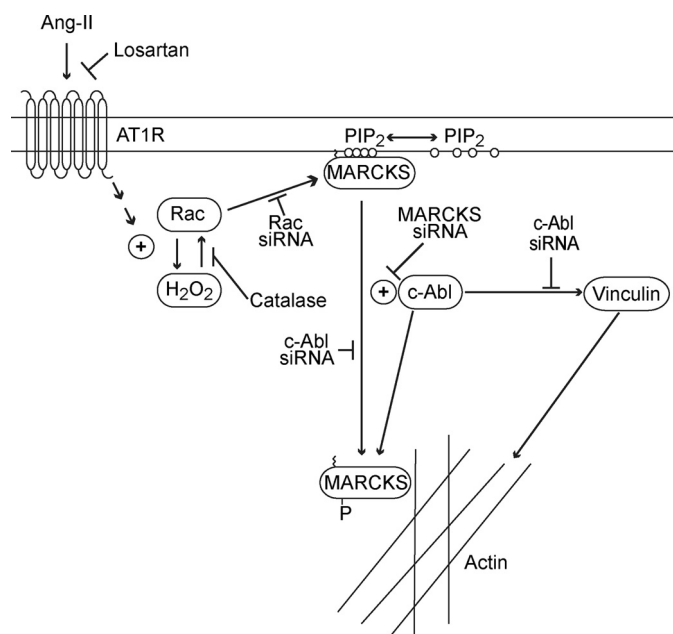
our studies in endothelial cells indicate that Rac1 is required for both Ang-II- as well as H_2O_2-dependent activation of MARCKS phosphorylation (Fig. 5), suggesting that Rac1 is downstream of at least some of the H_2O_2-modulated signaling responses in these cells (see *model* in Fig. 10). Rac1 clearly has pleiotropic roles in ROS metabolism. As a subunit of some membrane-targeted NADPH oxidase isoforms, Rac1 can directly participate in the synthesis of superoxide anion. Yet Rac1 is also a critical cytoskeleton regulatory GTPase that regulates key signaling proteins. The present studies have shown that H_2O_2 modulates Rac1-dependent signaling pathways that lead to MARCKS phosphorylation. The precise H_2O_2 metabolic pathway(s) that are modulated by Ang-II have not been identified in these studies, but our observations are not compatible with a major role for Rac1-dependent NADPH oxidase isoforms in mediating the Ang-II signaling responses seen in these cells.

Since the original classification of MARCKS as a protein kinase C (PKC) substrate, other protein kinases have also been implicated in MARCKS phosphorylation, including kinases that may themselves be subject to redox regulation. The increase in intracellular H_2O_2 that we observed following AT1 receptor activation may reflect either an increase in H_2O_2 syn-

thesis or a decrease in H_2O_2 degradation. The candidate enzymes include a broad range of differentially targeted signaling proteins that are involved in H_2O_2 metabolism, and which provide an alternative pathway for the receptor-dependent control of protein phosphorylation responses.

These studies provide new evidence for important links between signaling pathways that have largely been studied in isolation in previous reports. For example, the connections between Ang-II and ROS generation have been extensively characterized, but the critical involvement of MARCKS has not been previously appreciated. A connection between Ang-II and Rac1 activation has been observed, but the critical role for H_2O_2 in this pathway has not been previously described. The activation of MARCKS by receptor-regulated kinase pathways has been explored in earlier studies, but the involvement of neither Rac1 nor H_2O_2 in the MARCKS phosphorylation response has been previously reported. Thus, the present studies represent a synthesis of signaling pathways that previously were studied pairwise to now reveal distinctive features of an integrated signaling pathway that identify important new aspects of the vascular response to Ang-II.

Ang-II has been clearly implicated in vascular pathology, and drugs modulating angiotensin metabolism and angiotensin action are critical components in the therapeutic armamentarium for cardiovascular disease. The present studies have helped to establish that Ang-II and MARCKS are critical determinants of focal adhesion complex formation in cultured endothelial cells. It has long been known that Ang-II infusion in mice leads to the formation of aortic aneurysms (17), and a recent report showed that Ang-II-promoted aneurysm formation is attenuated in knock-out mice following targeted inactivation of the AT1 receptor specifically in vascular endothelial cells (20).

Our work has provided evidence for a signaling pathway in endothelial cells in which stimulation of the AT1 receptor leads to the elevation of intracellular H_2O_2 levels and to activation of the small GTPase Rac1, which are required for the subsequent phosphorylation and translocation of MARCKS, leading to an increase in localized PIP_2 levels and to the activation of kinase c-Abl, which is required for the recruitment of the PIP_2-sensitive protein vinculin, and lead ultimately to marked effects on cytoskeletal structure and cell adhesion. These observations that Ang-II and MARCKS so profoundly affect the cytoskeleton of aortic endothelial cells may provide a plausible mechanistic basis for understanding the derangements in Ang-II responses that lead to aneurysm formation. Further study of these pathways may lead to the identification of new sites for pharmacological intervention in disease states involving the vascular wall.

REFERENCES

1. Blackshear, P. J. (1993) The MARCKS family of cellular protein kinase C substrates. *J. Biol. Chem.* **268,** 1501–1504

2. Arnold, T. P., Standaert, M. L., Hernandez, H., Watson, J., Mischak, H., Kazanietz, M. G., Zhao, L., Cooper, D. R., and Farese, R. V. (1993) Effects of insulin and phorbol esters on MARCKS (myristoylated alanine-rich C-kinase substrate) phosphorylation (and other parameters of protein kinase C activation) in rat adipocytes, rat soleus muscle, and BC3H-1 myocytes. *Biochem. J.* **295,** 155–164

3. Arbuzova, A., Schmitz, A. A., and Vergeres, G. (2002) Cross-talk unfolded: MARCKS proteins. *Biochem. J.* **362,** 1–12

4. Lu, D., Yang, H., Lenox, R. H., and Raizada, M. K. (1998) Regulation of angiotensin II-induced neuromodulation by MARCKS in brain neurons. *J. Cell Biol.* **142,** 217

5. Shiraishi, M., Tanabe, A., Saito, N., and Sasaki, Y. (2006) Unphosphorylated MARCKS is involved in neurite initiation induced by insulin-like growth factor-I in SH-SY5Y cells. *J. Cell. Physiol.* **209,** 1029–1038

6. Yamaguchi, H., Shiraishi, M., Fukami, K., Tanabe, A., Ikeda-Matsuo, Y., Naito, Y., and Sasaki, Y. (2009) MARCKS regulates lamellipodia formation induced by IGF-I via association with PIP2 and β-actin at membrane microdomains. *J. Cell. Physiol.* **220,** 748–755

7. Finlayson, A. E., and Freeman, K. W. (2009) A cell motility screen reveals role for MARCKS-related protein in adherens junction formation and tumorigenesis. *PLoS One* **4,** e7833

8. Tzlil, S., Murray, D., and Ben-Shaul, A. (2008) The "electrostatic-switch" mechanism: Monte Carlo study of MARCKS-membrane interaction. *Biophys. J.* **95,** 1745–1757

9. Calabrese, B., and Halpain, S. (2005) Essential role for the PKC target MARCKS in maintaining dendritic spine morphology. *Neuron* **48,** 77–90

10. Gadi, D., Wagenknecht-Wiesner, A., Holowka, D., and Baird, B. (2011) Sequestration of phosphoinositides by mutated MARCKS effector domain inhibits stimulated Ca(2+) mobilization and degranulation in mast cells. *Mol. Biol. Cell* **22,** 4908–4917

11. Hussain, R. J., Stumpo, D. J., Blackshear, P. J., Lenox, R. H., Abel, T., and McNamara, R. K. (2006) Myristoylated alanine-rich C kinase substrate (MARCKS) heterozygous mutant mice exhibit deficits in hippocampal mossy fiber-CA3 long-term potentiation. *Hippocampus* **16,** 495–503

12. Kalwa, H., and Michel, T. (2011) The MARCKS protein plays a critical role in phosphatidylinositol 4,5-bisphosphate metabolism and directed cell movement in vascular endothelial cells. *J. Biol. Chem.* **286,** 2320–2330

13. Monahan, T. S., Andersen, N. D., Martin, M. C., Malek, J. Y., Shrikhande, G. V., Pradhan, L., Ferran, C., and LoGerfo, F. W. (2009) MARCKS silencing differentially affects human vascular smooth muscle and endothelial cell phenotypes to inhibit neointimal hyperplasia in saphenous vein. *FASEB J.,* **23,** 557–564

14. Tanabe, A., Shiraishi, M., Negishi, M., Saito, N., Tanabe, M., and Sasaki, Y. (2012) MARCKS dephosphorylation is involved in bradykinin-induced neurite outgrowth in neuroblastoma SH-SY5Y cells. *J. Cell. Physiol.* **227,** 618–629

15. Cai, H. (2005) Hydrogen peroxide regulation of endothelial function: origins, mechanisms, and consequences. *Cardiovasc. Res.* **68,** 26–36

16. Finkel, T. (2001) Reactive oxygen species and signal transduction. *IUBMB Life* **52,** 3–6

17. Mehta, P. K., and Griendling, K. K. (2007) Angiotensin II cell signaling: physiological and pathological effects in the cardiovascular system. *Am. J. Physiol. Cell Physiol.* **292,** C82–C97

18. Nathan, C. (2003) Specificity of a third kind: reactive oxygen and nitrogen intermediates in cell signaling. *J. Clin. Invest.* **111,** 769–778

19. Desideri, G., Bravi, M. C., Tucci, M., Croce, G., Marinucci, M. C., Santucci, A., Alesse, E., and Ferri, C. (2003) Angiotensin II inhibits endothelial cell motility through an AT1-dependent oxidant-sensitive decrement of nitric oxide availability. *Arterioscler. Thromb. Vasc. Biol.* **23,** 1218–1223

20. Rateri, D. L., Moorleghen, J. J., Balakrishnan, A., Owens, A. P., 3rd, Howatt, D. A., Subramanian, V., Poduri, A., Charnigo, R., Cassis, L. A., and Daugherty, A. (2011) Endothelial cell-specific deficiency of Ang II type 1a receptors attenuates Ang II-induced ascending aortic aneurysms in LDL receptor−/− mice. *Circ. Res.,* **108,** 574–581

21. Al Ghouleh, I., Khoo, N. K., Knaus, U. G., Griendling, K. K., Touyz, R. M., Thannickal, V. J., Barchowsky, A., Nauseef, W. M., Kelley, E. E., Bauer, P. M., Darley-Usmar, V., Shiva, S., Cifuentes-Pagano, E., Freeman, B. A., Gladwin, M. T., and Pagano, P. J. (2011) Oxidases and peroxidases in

cardiovascular and lung disease: new concepts in reactive oxygen species signaling. *Free Radic. Biol. Med.* **51,** 1271–1288

22. Apel, K., and Hirt, H. (2004) Reactive oxygen species: metabolism, oxidative stress, and signal transduction. *Annu. Rev. Plant Biol.* **55,** 373–399

23. Amanso, A. M., and Griendling, K. K. (2012) Differential roles of NADPH oxidases in vascular physiology and pathophysiology. *Front. Biosci.* **4,** 1044–1064

24. Garrido, A. M., and Griendling, K. K. (2009) NADPH oxidases and angiotensin II receptor signaling. *Mol. Cell. Endocrinol.* **302,** 148–158

25. Belousov, V. V., Fradkov, A. F., Lukyanov, K. A., Staroverov, D. B., Shakhbazov, K. S., Terskikh, A. V., and Lukyanov, S. (2006) Genetically encoded fluorescent indicator for intracellular hydrogen peroxide. *Nat. Methods* **3,** 281–286

26. Choi, H., Kim, S., Mukhopadhyay, P., Cho, S., Woo, J., Storz, G., and Ryu, S. E. (2001) Structural basis of the redox switch in the OxyR transcription factor. *Cell* **105,** 103–113

27. Markvicheva, K. N., Bilan, D. S., Mishina, N. M., Gorokhovatsky, A. Y., Vinokurov, L. M., Lukyanov, S., and Belousov, V. V. (2011) A genetically encoded sensor for H_2O_2 with expanded dynamic range. *Bioorg. Med. Chem.* **19,** 1079–1084

28. Sartoretto, J. L., Kalwa, H., Pluth, M. D., Lippard, S. J., and Michel, T. (2011) Hydrogen peroxide differentially modulates cardiac myocyte nitric-oxide synthesis. *Proc. Natl. Acad. Sci. U.S.A.* **108,** 15792–15797

29. Dietrich, U., Krüger, P., Gutberlet, T., and Käs, J. A. (2009) Interaction of the MARCKS peptide with PIP2 in phospholipid monolayers. *Biochim. Biophys. Acta* **1788,** 1474–1481

30. Aoki, K., Nakamura, T., Inoue, T., Meyer, T., and Matsuda, M. (2007) An essential role for the SHIP2-dependent negative feedback loop in neuritogenesis of nerve growth factor-stimulated PC12 cells. *J. Cell Biol.* **177,** 817–827

31. Sato, M., Ueda, Y., Takagi, T., and Umezawa, Y. (2003) Production of PtdInsP3 at endomembranes is triggered by receptor endocytosis. *Nat. Cell Biol.* **5,** 1016–1022

32. Gonzalez, E., Kou, R., and Michel, T. (2006) Rac1 modulates sphingosine 1-phosphate-mediated activation of phosphoinositide 3-kinase/Akt signaling pathways in vascular endothelial cells. *J. Biol. Chem.*, **281,** 3210–3216

33. Aoki, K., and Matsuda, M. (2009) Visualization of small GTPase activity with fluorescence resonance energy transfer-based biosensors. *Nat. Protoc.* **4,** 1623–1631

34. Aoki, K., Nakamura, T., and Matsuda, M. (2004) Spatio-temporal regulation of Rac1 and Cdc42 activity during nerve growth factor-induced neurite outgrowth in PC12 cells. *J. Biol. Chem.* **279,** 713–719

35. Itoh, R. E., Fujioka, A., Sharma, A., Mayer, B. J., and Matsuda, M. (2005) A FRET-based probe for epidermal growth factor receptor bound non-co-valently to a pair of synthetic amphipathic helixes. *Exp. Cell Res.* **307,** 142–152

36. Colicelli, J. (2010) ABL tyrosine kinases: evolution of function, regulation, and specificity. *Sci Signal.* **3,** re6

37. Schlatterer, S. D., Acker, C. M., and Davies, P. (2011) c-Abl in neurodegenerative disease. *J. Mol. Neurosci.* **45,** 445–452

38. Wang, B., E., Golemis, E. A., and Kruh, G. D. (1997) ArgBP2, a multiple Src homology 3 domain-containing, Arg/Abl-interacting protein, is phosphorylated in v-Abl-transformed cells and localized in stress fibers and cardiocyte Z-disks. *J. Biol. Chem.* **272,** 17542–17550

39. Zandy, N. L., and Pendergast, A. M. (2008) Abl tyrosine kinases modulate cadherin-dependent adhesion upstream and downstream of Rho family GTPases. *Cell Cycle* **7,** 444–448

40. Pluk, H., Dorey, K., and Superti-Furga, G. (2002) Autoinhibition of c-Abl. *Cell* **108,** 247–259

41. Izard, T., Evans, G., Borgon, R. A., Rush, C. L., Bricogne, G., and Bois, P. R. (2004) Vinculin activation by talin through helical bundle conversion. *Nature* **427,** 171–175

42. Yang, H. J., Chen, J. Z., Zhang, W. L., and Ding, Y. Q. (2010) Focal adhesion plaque associated cytoskeletons are involved in the invasion and metastasis of human colorectal carcinoma. *Cancer Invest.* **28,** 127–134

43. Blackshear, P. J., Lai, W. S., Tuttle, J. S., Stumpo, D. J., Kennington, E., Nairn, A. C., and Sulik, K. K. (1996) Developmental expression of MARCKS and protein kinase C in mice in relation to the exencephaly resulting from MARCKS deficiency. *Brain Res. Dev. Brain. Res.* **96,** 62–75

44. Sechi, A. S., and Wehland, J. (2000) The actin cytoskeleton and plasma membrane connection: PtdIns(4,5)P(2) influences cytoskeletal protein activity at the plasma membrane. *J. Cell Sci.* **113,** 3685–3695

45. Niethammer, P., Grabher, C., Look, A. T., and Mitchison, T. J. (2009) A tissue-scale gradient of hydrogen peroxide mediates rapid wound detection in zebrafish. *Nature* **459,** 996–999

46. Aoki, K., Kiyokawa, E., Nakamura, T., and Matsuda, M. (2008) Visualization of growth signal transduction cascades in living cells with genetically encoded probes based on Forster resonance energy transfer. *Philos. Trans R Soc. Lond. B Biol. Sci.* **363,** 2143–2151

47. Yoshizaki, H., Mochizuki, N., Gotoh, Y., and Matsuda, M. (2007) Akt-PDK1 complex mediates epidermal growth factor-induced membrane protrusion through Ral activation. *Mol. Biol. Cell* **18,** 119–128

48. Cowen, T., Haven, A. J., and Burnstock, G. (1985) Pontamine sky blue: a counterstain for background autofluorescence in fluorescence and immunofluorescence histochemistry. *Histochemistry* **82,** 205–208

49. Jin, B. Y., Sartoretto, J. L., Gladyshev, V. N., and Michel, T. (2009) Endothelial nitric oxide synthase negatively regulates hydrogen peroxide-stimulated AMP-activated protein kinase in endothelial cells. *Proc. Natl. Acad. Sci. U.S.A.* **106,** 17343–17348